Desalination 404 (2017) 147–154

Contents lists available at ScienceDirect

Desalination

journal homepage: www.elsevier.com/locate/desal

Calcium carbonate inhibition by green inhibitors: Thiamine and Pyridoxine

Rayane Menzri [a], Samira Ghizellaoui [a,*], Mohamed Tlili [b]

[a] Department of Chemical, University Constantine 1, Road Ain El Bey, 25000, Algeria
[b] Laboratory of Water Treatment, Center of Researches and Water Technologies, P.B 273, 8020 Soliman, Tunisia

HIGHLIGHTS

- The use of the mixture of vitamins leads to significant inhibition of calcium carbonate formation.
- The inhibition efficiency is around 66.78 % by the use of electrochemical impedance spectroscopy.
- The increase in the speed of precipitation of calcium carbonate overestimates the optimal amount of inhibitor.
- IR, X-ray diffraction and Raman spectroscopy analyses indicated modifications in crystalline structure.

ARTICLE INFO

Article history:
Received 28 February 2016
Received in revised form 1 November 2016
Accepted 5 November 2016
Available online 16 November 2016

Keywords:
Calcium carbonate
Green inhibitor
Scale formation
Calcite
Vaterite

ABSTRACT

In the East of Algeria, the city of Constantine called for its water supply, the Hamma groundwater resource. The high content of hydrogen carbonate and calcium justify the very important scaling power, it contains 82 % by mass of these ions.

This paper focuses on the application of a new green inhibitor "RS1600" for reducing calcium carbonate scale formation. RS1600 is a type of water soluble vitamin, it has proven to be green scale inhibitor given his nontoxic and biodegradable features. The inhibiting effect occurs at very low concentration. Its performance is evaluated and compared using different chemical and electrochemical anti-scaling methods.

The nucleation and scaling time were identified. The ratio between homogeneous and heterogeneous nucleation was determined. IR, X-ray diffraction and Raman spectroscopy analyses demonstrated modifications in crystalline structure, the $CaCO_3$ crystallize from calcite to vaterite. The study suggested that RS1600 is an excellent green chemical.

Contents

* Corresponding author.
E-mail address: gsamira@yahoo.com (S. Ghizellaoui).

http://dx.doi.org/10.1016/j.desal.2016.11.005
0011-9164/

1. Introduction

Hamma groundwater resource is a natural water, it contains scale-forming ions. The elevated concentration of HCO_3^- and Ca^{2+}, and important water temperature cause the scale formation by calcium carbonate, one of the most common scale components found in cooling water systems [1,2], oilfield production [3] and desalination units [4].

Deposits formation may cause severe corrosion and deteriorate conditions of the heat exchange [1]. The most common and effective scale control method is the addition of small concentrations of inhibitors to the water [5–8]. Thus, the concept of "green chemistry" was proposed, and green scale inhibitors have become an important focus in water treatment technology [9,10]. All the last researches [1,10–13] have proved that the addition of scale inhibitors induce morphological changes of the crystal shape.

In pursuance of going greener, we investigated the scale inhibiting of RS1600 which is a novel scale inhibitor and shows promising prospect as a green water-treatment agent for circulated cooling water. RS1600 is the mixture of two vitamins: Thiamine (50 %) and Pyridoxine (50 %). The chemicals formula of their vitamins are: $C_{12}H_{17}ClN_4OS$ and $C_8H_{11}NO_3$.

In the present study, we evaluated the physico-chemical quality of the hard water of Hamma and inhibit the furring power of these waters by the use of different chemical and electrochemical scaling methods. Formed scales were characterized by: IR, XRD and Raman spectroscopy. The result shows that the RS1600 changed the morphology of $CaCO_3$ precipitates.

2. Materials and methods

2.1. The precipitation of $CaCO_3$ by degassing dissolved-CO_2 method

It was first developed in 1994 by Roques et al. [14] and it has been used in many studies [15–17,4]. Its principle is based on the displacement of the calcocarbonic equilibrium in the direction of the precipitation of $CaCO_3$ by degassing dissolved-CO_2, as the equation of the following reaction shows:

$$Ca^{2+} + 2HCO_3^- \leftrightarrow CaCO_3 + H_2O + CO_2 \quad (1)$$

Thus, it allows to control the changes in the concentration of dissolved-CO_2 which is the main motor of the system evolution leading to scaling [18].

In this first part, we were used the technique of degassing the dissolved-CO_2 by stirring [19], and the results were checked by a second method it is the technique of degassing the dissolved-CO_2 by the nitrogen sparge.

In the precipitation test, 500 mL of no-treated and treated water was placed in a stainless steel cell and immersed in thermostatic water bath to maintain 30 °C. According to Karoui et al. [4], during the precipitation test, the pH of the solution was continuously recorded. Samples of 1 mL were withdrawn from the solution and their HCO_3^- ion concentration was analysed by sulphuric acid (10^{-2} M) in the presence of the bromochrizole green (as indicator). At the end of the treatment, precipitate was recovered by filtration on a 0,45 μm pore size cellulose nitrate membrane. According to Alimi et al. [17], we can deduced from the calcium carbonate mass m_b formed in the bulk of the solution by homogeneous nucleation and the initial calcium carbonate mass m_0, the mass of calcium carbonate m_w deposited on the walls of the cell by heterogeneous nucleation.

2.1.1. CO_2 degasification by agitation

After a regular agitation of 800 rev/min by a magnetic stirrer to the solution of 500 mL, the degasification of the dissolved-CO_2 occurs.

The schema of the experimental setup is presented in Fig. 1.

2.1.2. CO_2 degasification by nitrogen sparge

In this technique, the CO_2 degasification was provoked by a continuous flow of pure nitrogen (8 L/min) through a diffuser located at the bottom of the cell.

We have chosen to work with a stainless steel cell because it is the same material that was used for the previous technique.

The diagrammatic representation of the system is shown in Fig. 2.

2.1.3. Chronoamperometry

Chronoamperometry, is one of the electrochemical method proposed by Ledion et al. [20]. The principle is to cover with calcium carbonate a metal surface carried to a fixed negative potential (−1 V versus SCE), corresponding to the limiting current of the reduction reaction of the dissolved oxygen:

$$O_2 + 4e^- + 2H_2O \rightarrow 4OH^- \quad (2)$$

By increasing the local pH in the vicinity of the metal surface where O_2 is reduced [21], the hydroxide ions promote the calcium carbonate to precipitate according to the chemicals reactions:

$$HCO_3^- + OH^- \rightarrow CO_3^{2-} + H_2O \text{ (in bulk)} \quad (3)$$

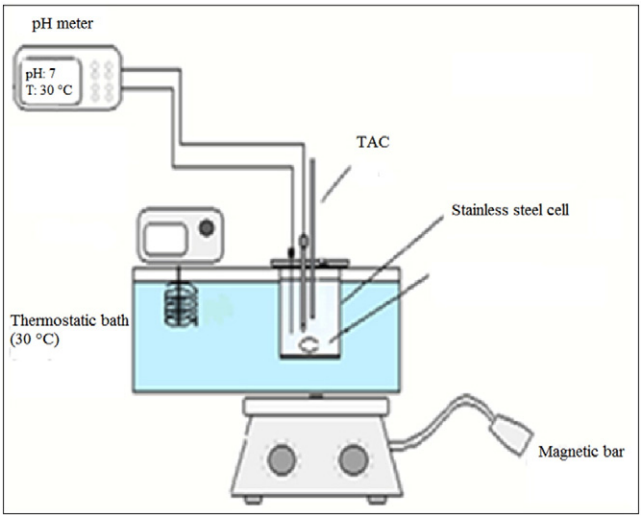

Fig. 1. Experimental setup scaling accelerated by agitation.

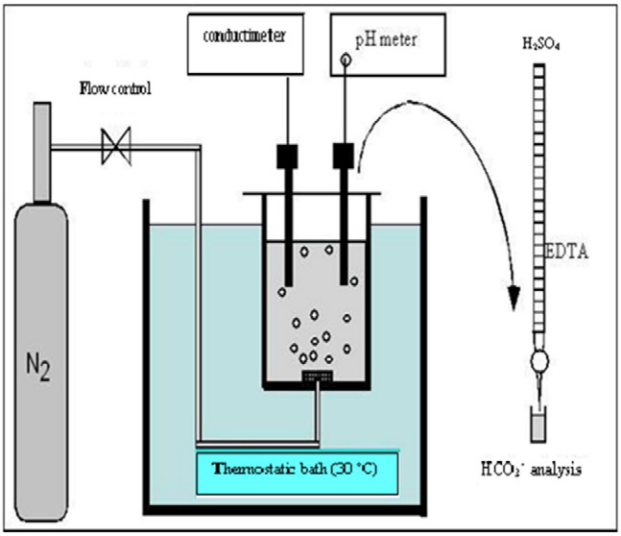

Fig. 2. Experimental setup scaling accelerated by nitrogen bubbling.

$$Ca^{2+} + CO_3{}^{2-} \rightarrow CaCO_3 \text{ (at the interface)} \quad (4)$$

Gabrielli et al. [22], defined the scaling time, t_s, as the time needed to reduce the current to practically zero. It is the intersection of the tangent at the inflexion point of the curve and the time axis according to [20]. The active area of the electrode reduced by the formed deposit, therefore the total cathodic current decreases [23].

The more compact and insulating the scale, the lower the residual current [24].

Electrochemical experiments were carried out under potentiostat condition using AUTO LAB potentiostat. A computer provided with windows software application (VoltaMaster 4) was used.

The schema of the experimental arrangement is presented in Fig. 3.

The working electrode is made of steel XC10 with 1.003 cm^2 area. The electrode surface was polished with silicon carbide paper (p1200), rinsed thoroughly with distilled water and carefully dried.

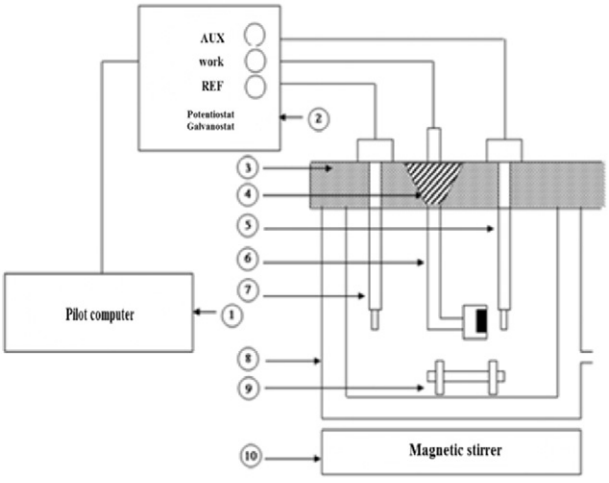

Fig. 3. Experimental setup. 1 - Pilot computer 2 - Potensiostat-galvanostat 3 - Cover electrode holder 4 - Cap sample holder 5 - Platinum electrode 6 - Sample: steel pelle XC10 (1.003 cm) embedded in an inert resin 7 - Reference electrode Calomel saturated KCl 8 - Glass beaker of 600 mL 9 - Magnetic bar 10 - Magnetic stirrer.

Table 1
Hamma water analysis.

The parameters	Water of Hamma	WHO standards
T °C	30	25
pH	7.16	6.5–8.5
CE mS/cm	1	1.25
RS mg/L	680	–
HCO_3^- mg/L	412	200
Ca^{2+} mg/L	146	100
Mg^{2+} mg/L	45	50
Na^+ mg/L	83	200
K^+ mg/L	3	–
Cl^- mg/L	144	250
SO_4^{2-} mg/L	160	500
NO_3^- mg/L	8.8	50
F^- mg/L	0.21	1.5
PO_4^{3-} mg/L	1.02	–
NO_2^- mg/L	0.01	0

2.2. Electrochemical impedance

Electrochemical impedance spectroscopy (EIS) measurements were carried out using Gamry 3000 instrument. A constant potential of −1 V/SCE (saturated calomel electrode) was applied to the working electrode.

3. Results and discussion

3.1. Physico-chemical characterization of Hamma groundwater

The physico-chemical characterization of the different parameters is an essential step. It gives a clear idea about the elements that are responsible for the scaling phenomenon. The results are given in Table 1.

As a first reading in the chemical composition, we see a rise in temperature, it is 30 °C. Thus, a high content of hydrogen carbonate (412 mg/L) and calcium (146 mg/L), therefore this water contains 82 % by mass of these ions. These three parameters justify the very important scale forming of this water.

On the other hand, according to this Table, the content of the other parameters is very moderate and does not exceed the WHO standards.

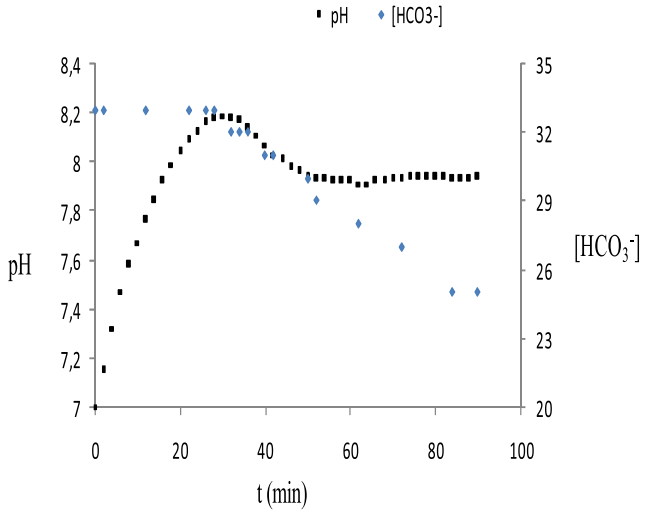

Fig. 4. Variation of the pH and [HCO_3^-] with degasification time for Hamma water at 30 °C and 800 rev/min.

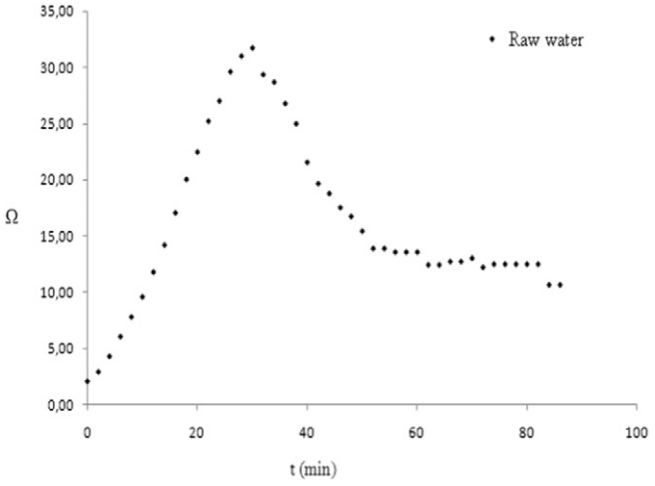

Fig. 5. Evolution of the supersaturation coefficient.

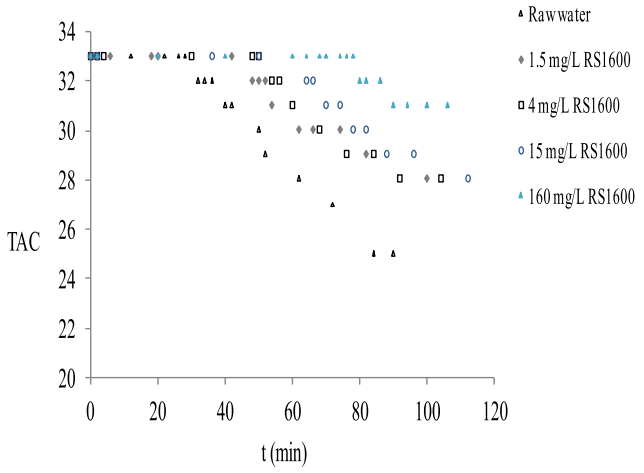

Fig. 7. Evolution of TAC versus time and RS1600 amount added at 30 °C (800 rev/min).

3.2. CO_2 degasification by agitation

Before performing the precipitation tests on our water, we set the initial pH to 7 by simply bubbling CO_2 gas in the solution. The changing calcocarbonic system over time is monitored by the continuous measurement of pH and [HCO_3^-].

The results are shown in Figs. 4 and 5 for the raw water.

At the beginning of the experiment, the solution is rich in CO_2, the greater the degasification, the lower increases pH.

It is noted that the increase in pH is very fast up to 30 min through a maximum at pH = 8.19 (Fig. 4). Another maximum is observed on the curve of the supersaturation coefficient: Ω = 31.73 (Fig. 5).

Up to 30 min, no precipitation was detected by determination of HCO_3^- ions, which is indicated by the landing of germination on the [HCO_3^-] curve.

From the beginning of the experiment, the solution is supersaturated relatively to calcite, the thermodynamically most stable phase [25] ($\Omega_{pH=7} = 2.05$) but the threshold nucleation is achieved when the solution is in a state of saturation of: $\Omega_{pH=8.19} = 31.73$. The pH of the solution decreases after having reached the maximum value.

This state of metastability abruptly ceases at nucleation time t_n, the time necessary to form the first calcium carbonate nuclei in the solution. It first manifested on the pH which shows a change in the slope. This change can be related with the protons release when the crystal growth starts according to Eq. (5):

$$Ca^{2+} + HCO_3^- + H_2O \leftrightarrow CaCO_3 + H_3O^+ \quad (5)$$

For Guillaume Gauthier et al. [26] these evolutions indicate a massive precipitation of $CaCO_3$, that is accompanied by a fall in the bicarbonate ions (Fig. 4). At the start of the crystal growth, the precipitation rate is fast. At the end of the experiment, the system evolves more slowly to reach an equilibrium state at [HCO_3^-] = 25 °F: landing final precipitation.

At this stage corresponding to the period of high speed, the release speed of H^+ released by reaction (5), outweighs the consumption rate of these same H^+ according to Eq. (6) and on the venting speed of formed CO_2, therefore decreasing in pH.

$$H_3O^+ + HCO_3^- \leftrightarrow CO_2 + 2H_2O \quad (6)$$

Beyond 60 min, the rate of precipitation decreases, the trend reversed and after a minimum, the pH starts to grow slightly.

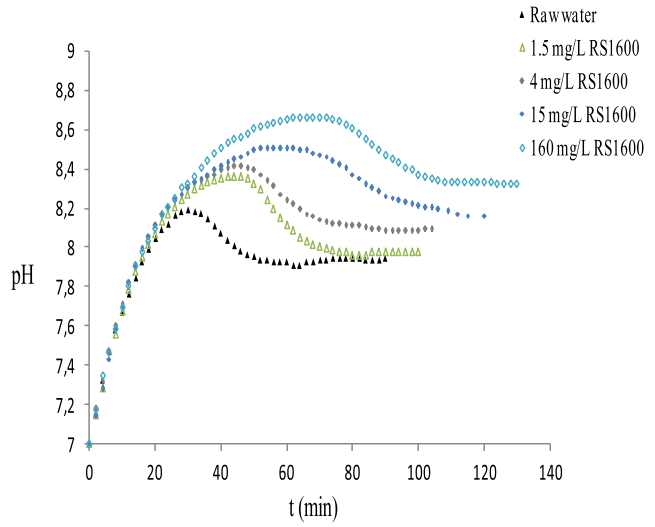

Fig. 6. Evolution of pH versus time and RS1600 amount added at 30 °C (800 rev/min).

3.2.1. Optimization of RS1600

The RS1600 was added at different concentrations in the solution at 30 °C, to optimize the effective concentration for the scaling prevention. Figs. 6 and 7 show the changes of the pH and [HCO_3^-] with time for Hamma water without and with varying concentrations of RS1600.

The nucleation time increases from 30 min for the raw water to 46 min with 4 mg/L RS1600 to attain 72 min at a concentration of 160 mg/L, for the latter concentration the precipitation ratio decreases from 24.24 % to 6.06 %, which corresponds a reduction of 18 % compared to the solution without inhibitor. Thus, we notice that the crystalline growth rate decreases 3 times. Our results are in good agreement with the results of Tlili et al. [16], they showed the same phenomenon with another inhibitor. Therefore this new inhibitor prove his inhibitory effect, it can delay the nucleation time and subsequently prolong the degassing phase, although the supersaturation coefficient is very high

Table 2
Variation of t_n, pH_n, Ω_n, τ, %hm, %ht, Ḱ, and P_{CO_2} as a function adding RS1600.

RS1600 (mg/L)	t_n	pH_n	Ω_n	τ	%hm	%ht	Ḱ	P_{CO_2}
0	30	8.19	31.73	24.24	2.33	97.66	$13.6 \cdot 10^{-2}$	$2.65 \cdot 10^{-3}$
1.5	42	8.36	46.93	15.15	2.30	97.69	$7.8 \cdot 10^{-2}$	$1.79 \cdot 10^{-3}$
4	46	8.41	52.65	15.15	2.25	97.74	$6.8 \cdot 10^{-2}$	$1.59 \cdot 10^{-3}$
15	62	8.5	64.78	15.15	1.84	98.15	$5.6 \cdot 10^{-2}$	$1.29 \cdot 10^{-3}$
160	72	8.66	93.63	6.06	1.6	98.40	$4.6 \cdot 10^{-2}$	$8.98 \cdot 10^{-4}$

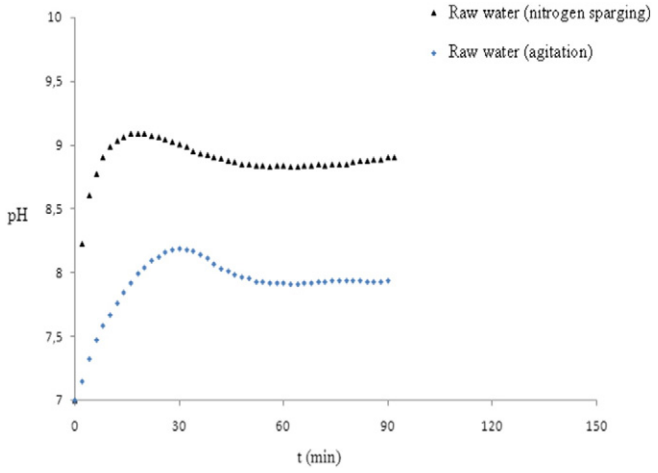

Fig. 8. Influence of the CO_2 degassing rate on the pH evolution for raw water.

$\Omega = 93.63$ compared to $\Omega = 31.73$ for the raw water and the value of $P_{CO_2} = 8.9 \cdot 10^{-4}$ atm which is very close to the working gas $P_{CO_2} = 3 \cdot 10^{-4}$ atm.

Let us note that the presence of this inhibitor actually increase the percentage of the heterogeneous precipitation, therefore the amount of deposited scale on the walls.

Table 3
Variation of t_n, pH_n, Ω_n, Ḱ, and P_{CO_2} for raw water.

	t_n	pH_n	Ω_n	Ḱ	P_{CO_2}
Degassing by agitation	30	8.19	31.73	$13.6 \cdot 10^{-2}$	$2.65 \cdot 10^{-3}$
Degassing by nitrogen sparging	20	9.09	252.01	$24.5 \cdot 10^{-2}$	$3.33 \cdot 10^{-4}$

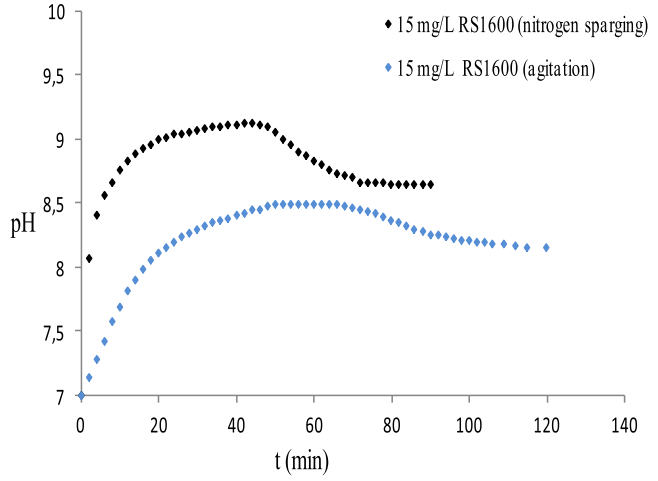

Fig. 9. Influence of the rate of evolution of CO_2 on the pH evolution for treated water by RS1600.

Table 4
Variation of t_n, pH_n, Ω_n, Ḱ, et P_{CO_2} for treated water.

	t_n	pH_n	Ω_n	Ḱ	P_{CO_2}
Degassing by agitation (15 mg/L)	62	8.5	64.78	$5.9 \cdot 10^{-2}$	$1.29 \cdot 10^{-3}$
Degassing by bubbling nitrogen (15 mg/L)	44	9.13	276.33	$30.5 \cdot 10^{-2}$	$3.04 \cdot 10^{-4}$

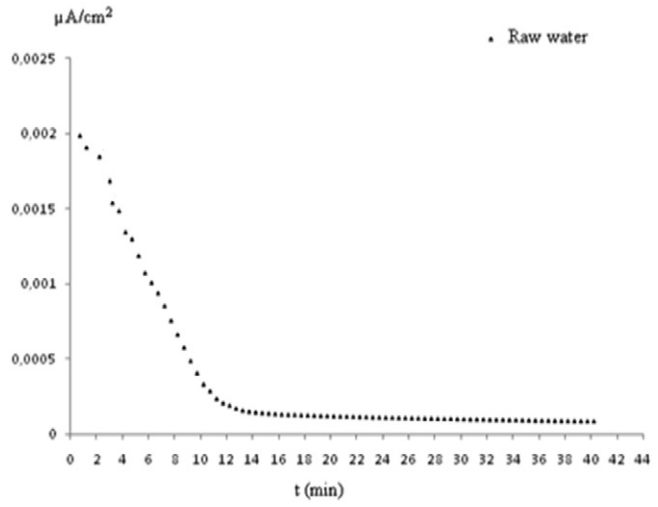

Fig. 10. Chronoamperometric curve of Hamma raw water at 30 °C.

In Table 2 are illustrated the influence of RS1600 on the: t_n, pH_n, Ω_n, τ, %hm, %ht, Ḱ, and P_{CO_2}. Such as:

- t_n: the nucleation time.
- pH_n: the pH at the nucleation time.
- Ω_n: the supersaturation coefficients were determined at $t = t_n$. It depends on the (Ca^{2+}) and (CO_3^{2-}) activity according to:

$$\Omega = \frac{(Ca^{2+})\left(CO_3{}^{2-}\right)}{K_s}$$

where K_s is the solubility constant of calcium carbonate.

- τ: the precipitation ratio. It was determined from the following equation:

$$\tau = \frac{TAC_0 - TAC_t}{TAC_0} * 100$$

where: TAC_0 is the TAC at $t = 0$ min and TAC_t is the TAC at the end of precipitation test.

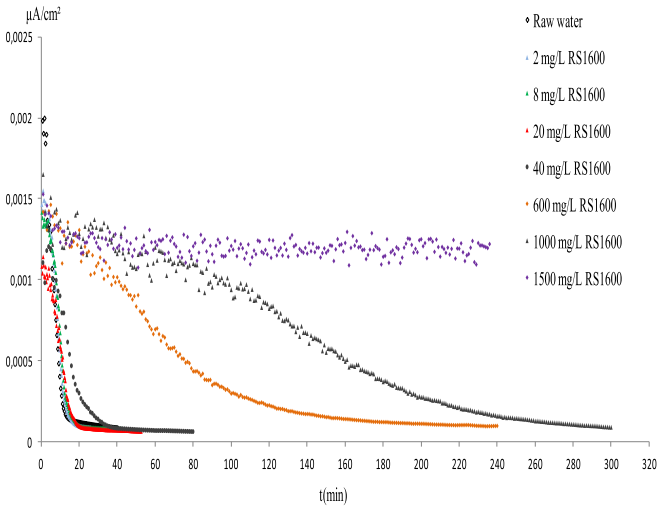

Fig. 11. Chronoamperometic curves in Hamma water with different concentrations of RS1600.

Table 5
Evolution of the scaling time in the presence of RS1600 at 30 °C.

Concentration (mg/L)	t_s (min)
0	12
2	13.3
8	15
20	18
40	26
600	135
1000	240
1500	∞

- %hm: the percentage of the homogeneous precipitation.
- %ht: the percentage of the heterogeneous precipitation.
- Ḱ: the crystalline growth rate. It was determined from the slope of the linear part of the precipitation curve.
- P_{CO_2}: CO_2 pressure in the solution.

3.3. Precipitation of $CaCO_3$ by CO_2 degassing by bubbling nitrogen

To make a comparison between the precipitation of $CaCO_3$ by CO_2 degassing by agitation and the precipitation of $CaCO_3$ by CO_2 degassing by nitrogen sparging, we have chosen to take a single concentration of each inhibitor, which allowed us to highlight the influence of CO_2 degassing speed on the threshold germination of $CaCO_3$.

3.3.1. Superposition of curves for Hamma hard water without inhibitor

The results of the pH evolution during the precipitation of the 2 tests are shown in Fig. 8 and Table 3.

It appears in Table 3 that the nucleation time is very influenced by the mode of CO_2 degassing, it goes from 30 min to 20 min. The nucleation occurred at pH increasingly higher and consequently the supersaturation coefficients increasingly strong. The pH increased from 8.19 for $\Omega = 31.73$ to pH = 9.09 for $\Omega = 252.01$, this is due to the increase in degassing speed by a factor of 2.

Table 6
Electrochemical impedance results in the presence of RS1600 at 30 °C.

Concentration (mg/L)	R_t (Ω/cm^2)	C_d (μF/cm^2)$*$ 10^{-6}	% of inhibition
0	9197	40.45	–
8	5560	104.4	39.54
20	3800	133.6	58.68
40	3055	162.7	66.78

3.3.2. Superposition of curves for treated water

Fig. 9 shows the pH evolution during the precipitation of two tests with the green inhibitor, and Table 4 summarizes the results that characterize their statements.

Seen the results shown in Table 4, we found that: precipitation of tarte can be provoked by the two methods of accelerated degassing and from these results we can rank the effectiveness of our inhibitor, which is made on the basis of the values of t_n. Indeed, the more t_n, the higher the inhibitor is effective. The problem is the overestimation of content using the method of CO_2 degassing by nitrogen bubbling.

For this same concentration of RS1600, pH increases from 8.5 (degassing by agitation) to 9.13 (degassing by bubbling nitrogen), unlike the nucleation time passes from 62 min to 44 min, as far as the coefficient of supersaturation that reaches a very high value of 276.33, this can be explained by the increase of the degassing speed by a factor of 5.

3.4. Scaling power

3.4.1. Optimization of RS1600

Chronoamperometric curve from Hamma water is presented in Fig. 10 at 30 °C. It is clearly observed that the current decreases, as the active electrode surface is progressively blocked by the precipitation of $CaCO_3$. The scaling time is reached when this surface is completely covered by this layer of scale.

For Hamma hard water, $t_s = 12$ min and $I_S = 83.33$ min^{-1}, so this water is a very scale-forming according to the classification of [20].

With the aim to evaluate the scale inhibitor efficiency, various quantities of RS1600 were introduced in our water. Fig. 11 presents the current evolution versus time in the presence of RS1600. The study of the curves showed that for raw water the scaling time was 12 min and in

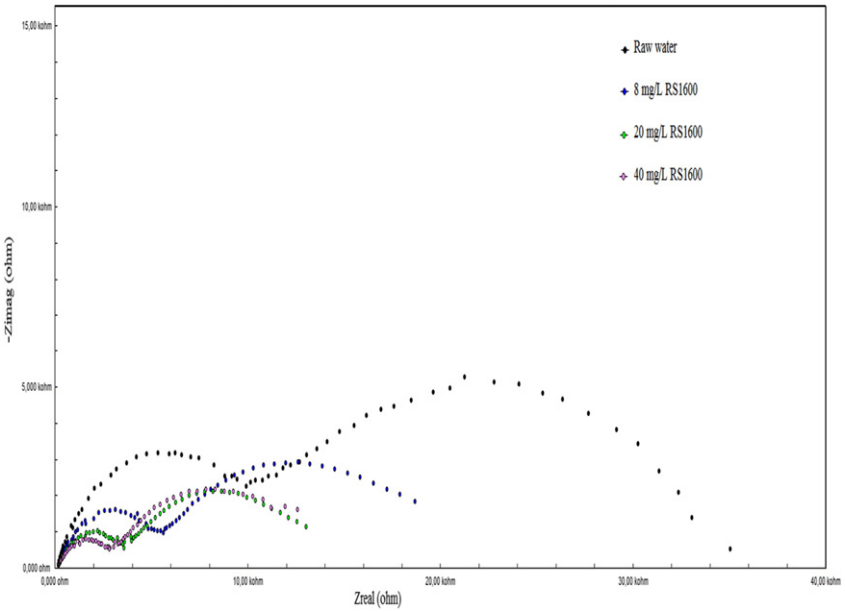

Fig. 12. Nyquist plot obtained after $CaCO_3$ scaling with different quantities of RS1600.

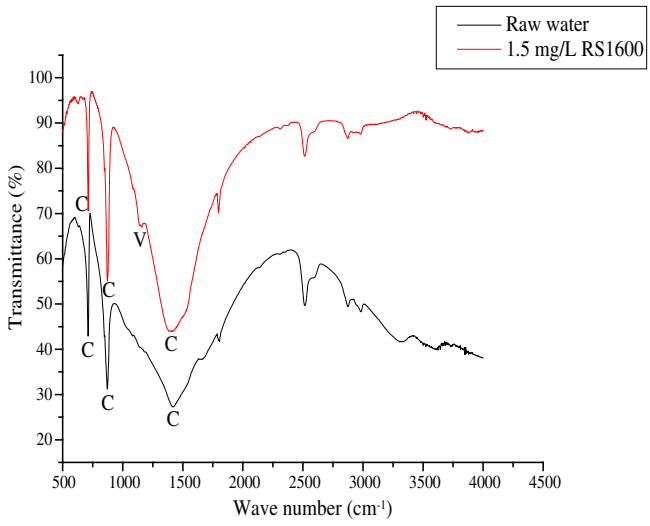

Fig. 13. FTIR spectra of precipitated scale products in absence and presence of 1.5 mg/L of RS1600.

the presence of 40 mg/L of RS1600 became 26 min. Therefore, it increases 2 times.

In the presence of 1500 mg/L, no scale was detected on the electrode surface, the curve becomes practically a line. In conclusion, 1500 mg/L of RS1600 is the most effective amount and this inhibitor can be used as a good antiscalant. In Table 5 are illustrated the evolution of the scaling time in the presence of RS1600 at 30 °C.

3.5. Electrochemical impedance

The impedance diagram recorded at the high frequency region for solutions with and without inhibitor is presented in Fig. 12. The Nyquist plots were used to determine the charge transfer resistance values (R_t) and the double layer capacitance values (C_d). The results are presented in Table 6.

The R_t value for raw water is 9197 Ω/cm^2, and for 8 mg/L of RS1600 the R_t value is drastically decreased to 5560 Ω/cm^2. But for the adding of 20 mg/L and 40 mg/L of RS1600, the charge transfer resistance is slowly decreased to 3055 Ω/cm^2. Conversely, the double layer capacitance values are increased from 40.45 μF/cm^2 to 162.7 μF/cm^2 due to the inhibition of the scale by this inhibitor. The inhibition efficiency is around 66.78 %.

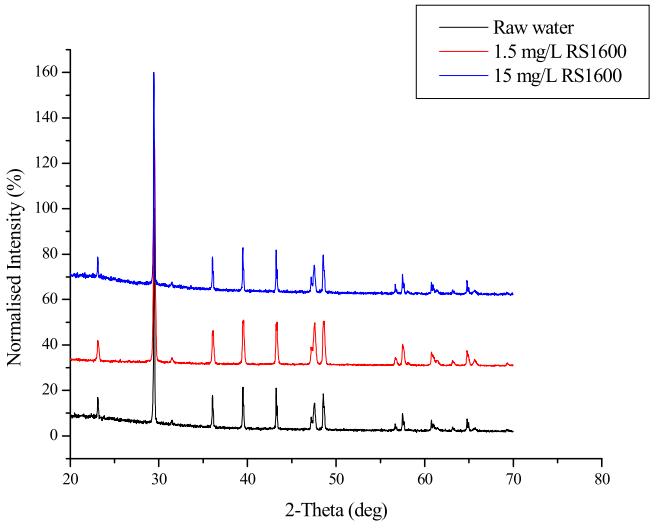

Fig. 14. XRD pattern of precipitated scale products in absence and presence of 1.5 mg/L and 15 mg/L of RS1600.

3.6. Characterization of scale

3.6.1. Interpretation of FTIR data

Fig. 13 shows the Fourier transformed infrared (FTIR) spectra of precipitated scale products in absence and presence of 1.5 mg/L RS1600. For raw water, the peaks at 711 cm^{-1}, 1430 cm^{-1}, 875 cm^{-1} (plane bending and asymmetric stretching) reflect the feature of calcite (C) which is the most thermodynamically stable. In the presence of RS1600 the calcium carbonate precipitate is the mixture of calcite and vaterite (V) with other characteristic band at ~1085 cm^{-1}. This confirmed that calcite showed tendency to get transformed into vaterite, the least stable form in the three polymorphic forms of calcium carbonate [27].

3.6.2. Interpretation of XRD data

The precipitated phases were identified by X-ray diffraction (XRD), which is a very important tool for identification and confirmation of crystalline forms [28], and the spectra are shown in Fig. 14.

This figure shows that in the absence of RS1600, calcite is the main crystal form (2θ = 23.12°, 29.45°, 36.06°, 39.49°, 43.25°) but in the presence of RS1600 the diffractogram showed a binary mixture of calcite and vaterite (2θ = 10.97° in the presence of 1.5 mg/L RS1600 and 2θ =20.81°, 17.21° in the presence of 15 mg/L RS1600).

Table 7 shows the crystallographic parameters obtained from the XRD studies of the scale products in absence and presence of RS1600. It could be seen that: peak position (PP) and peak intensity (PI) values are not exactly same, indicating difference in crystal morphology between inhibited and uninhibited crystals. The reduction in the peak intensity (PI) for diffraction peaks at 23.12° and 43.25° of calcite phase in the presence of RS1600 may indicate deviation from hexagonal crystal structure of calcite and decrease in adherence property [13].

3.6.3. Interpretation of Raman spectroscopy

The above results were further confirmed by Raman spectroscopy (Fig. 15) the characteristic symmetric stretching band at 1085 cm^{-1}, the lattice modes at 153 cm^{-1} with overlapping band at 281 cm^{-1} and band at 711 cm^{-1} confirmed the presence of calcite in the absence of inhibitor. The lattice band at 212 cm^{-1} confirmed the presence of vaterite in the presence of 15 mg/L RS1600.

Table 7
Peak position (PP) and peak intensity (PI) values in absence and presence of RS1600.

Without RS1600		With 1.5 mg/L RS1600		With 15 mg/L RS1600	
PP	PI	PP	PI	PP	PI
23.12	720.17	9.02	300.22	16.92	493.01
29.45	4274.43	10.97	389.00	17.21	490.45
36.06	750.44	23.12	560.56	18.04	493.38
39.49	913.84	29.48	4760.36	19.73	474.53
39.60	481.00	36.12	777.03	20.81	460.93
43.25	878.79	39.55	964.43	21.64	444.62
47.19	356.91	43.25	861.18	23.12	433.02
47.56	614.02	47.20	380.50	29.44	3849.00
48.56	778.30	47.58	926.83	36.05	725.14
56.67	221.95	48.60	949.18	36.15	465.00
56.83	169.09	48.64	960.83	39.48	904.85
57.51	413.16	56.68	214.69	39.58	519.80
57.65	261.77	57.52	486.14	43.25	840.83
60.77	298.17	60.78	316.94	47.19	385.26
60.94	210.69	64.79	350.59	47.54	584.01
64.79	316.13	64.94	274.09	48.55	762.03
–	–	–	–	56.68	262.33
–	–	–	–	57.51	427.13
–	–	–	–	60.77	296.87
–	–	–	–	64.78	324.81

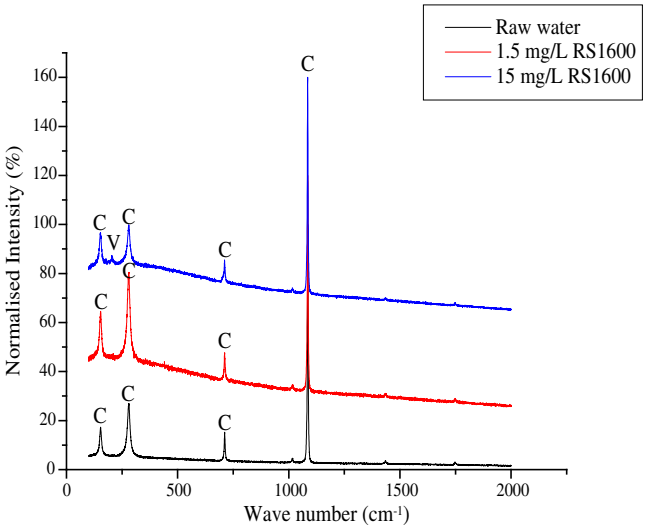

Fig. 15. Raman spectra of precipitated scale products in absence and presence of 1.5 mg/L and 15 mg/L of RS1600.

4. Conclusion

The most widely used medium to prevent the formation of scale deposits till now is chemical inhibition, but remains to be verified the closest to the real case optimization method, for it we selected four methods for rapid precipitation of $CaCO_3$:

- degassing of CO_2 by stirring
- degassing of CO_2 by nitrogen bubbling
- chronoamperometry
- electrochemical impedance spectroscopy.

Our study clearly defines the causes leading to the scaling with the physico-chemical characterization of our water (a high content of HCO_3^- and Ca^{2+}, in addition an elevated temperature).

The results show that the formation of $CaCO_3$ can be performed by the four techniques accelerated precipitation. These techniques have shown that RS1600 capable to delay the germination kinetics with a nucleation time equal to 72 min in the presence of 160 mg/L, by the method of degassing of CO_2 by stirring. In addition, the CO_2 degassing by bubbling nitrogen shows the need to increase the content for the inhibitor to inhibit the germination crystals, while the optimization by the use of chronoamperometry overestimates more contents optimal, hence these results are very far from reality. The main cause is the increase in the speed of precipitation of calcium carbonate. This can lead to adverse effects for the life of living beings and for the environment, in addition to financial losses. The inhibition efficiency is around 66.78 % by the use of electrochemical impedance spectroscopy. The interpretation of FTIR, XRD and Raman spectroscopy demonstrated modifications in crystalline structure. The use of a novel inhibitor considered a green product intended to treat drinking water showed its effectiveness.

References

[1] C. Wang, S.-P. Li, T.-d. Li, Calcium carbonate inhibition by a phosphonate-terminated poly(maleic-co-sulfonate), Desalination 249 (2009) 1–4.
[2] K. Chauhan, R. Kumar, M. Kumar, P. Sharma, G.S. Chauhan, Modified pectin-based polymers as green antiscalants for calcium sulfate, Desalination 305 (2012) 31–37.
[3] Y. Zhang, H. Shaw, R. Farquhar, R. Dawe, The kinetics of carbonate scaling, J. Pet. Sci. Eng. 29 (2001) 85–95.
[4] H. Karoui, M.M. Tlili, B. Riffault, M. Ben Amor, H. Mosrati, R. Mosrati, O. Gil, Influence of clay suspensions on the precipitation of $CaCO_3$ in seawater, Cryst. Res. Technol. 45 (2010) 259–266.
[5] H.Y. Li, W. Ma, L. Wang, R. Liu, L.S. Wei, Q. Wang, Inhibition of calcium and magnesium-containing scale by a new antiscalant polymer in laboratory tests and a field trial, Desalination 196 (2006) 237–247.
[6] I. Atamanenko, A. Kryvoruchko, L. Yurlova, E. Tsapiuk, Study of the $CaSO_4$ deposits in the presence of scale inhibitors, Desalination 147 (2002) 257–262.
[7] S. Ghizellaoui, Partial elimination of the water hardness by using (lime, soda and sodium carbonate): representation of calcocarbonic balance curves, Eur. J. Water Qual. 43 (2012) 117–132.
[8] R. Menzri, S. Ghizellaoui, Chronoamperometry study of the inhibition of groundwater scaling deposits in Fourchi, Energy Procedia 18 (2012) 1523–1532.
[9] A. Martinod, M. Euvrard, A. Foissy, A. Neville, Progressing the understanding of chemical inhibition of mineral scale by green inhibitors, Desalination 220 (2008) 345–352.
[10] Z. Belarbi, J. Gamby, L. Makhloufi, B. Sotta, B. Tribollet, Inhibition of calcium carbonate precipitation by aqueous extract of *Paronychia argentea*, J. Cryst. Growth 386 (2014) 208–214.
[11] D. Liu, W. Dong, F. Li, F. Hui, J. Ledion, Comparative performance of polyepoxysuccinic acid and polyaspartic acid on scaling inhibition by static and rapid controlled precipitation methods, Desalination 304 (2012) 1–10.
[12] Y. Xu, B. Zhang, L. Zhao, Y. Cui, Synthesis of polyaspartic acid/5-aminoorotic acid graft copolymer and evaluation of its scale inhibition and corrosion inhibition performance, Desalination 311 (2013) 156–161.
[13] T. Kumar, S. Vishwanatham, S.S. Kundu, A laboratory study on pteroyl-L-glutamic acid as a scale prevention inhibitor of calcium carbonate in aqueous solution of synthetic produced water, J. Pet. Sci. Eng. 71 (2010) 1–7.
[14] H. Roques, L. Dedieu, C. Hort, A. Martin-dominguez, M. Rola, Contribution à l'étude des phénomènes d'entartrage: Généralité et méthode d'étude LCGE, Tribune de l'eau 571/5 (1994).
[15] H. Elfil, Contribution à l'étude des eaux géothermales du sud tunisien, 1.N.S.A de Toulouse, N0507, France, 1999.
[16] M. Tlili, H. Elfil, M. Ben Amor, L'inhibition chimique de l'entartrage: détermination de la concentration efficace d'inhibiteurs par les techniques LCGE et CEG, Cahier de l'association Scientifique Européenne pour l'eau et la santé Volume 6 (N 1) (2001) 29–39.
[17] F. Alimi, M. Tlili, C. Gabrielli, M. Georges, M. Ben Amor, Effect of a magnetic water treatment on homogeneous and heterogeneous precipitation of calcium carbonate, Water Res. 40 (2006) 1941–1950.
[18] M. Tlili, étude des mécanismes de précipitation de carbonate de calcium. Application à l'entartrage, (Thèse de doctorat), Université de Sfax, Tunisie, 2002.
[19] J. Ledion, S. Mabrouk, E. Sezee, H. Julien, Modification du pouvoir entartrant de l'eau par chauffage micro-ondes, J. Eur. Hydrol. 30 (1999) 13–34.
[20] J. Ledion, P. leroy, J.-P. labbe, Détermination du caractère incrustant d'une eau par un essai d'entartrage accéléré. TSM L'eau, Juillet–Août 1985 323–328.
[21] C. Gabrielli, M. Keddam, G. Maurin, H. Perrot, R. Rosset, M. Zidoune, Estimation of the deposition rate of thermal calcareous scaling by the electrochemical impedance technique, J. Electroanal. Chem. 412 (1996) 189–193.
[22] C. Gabrielli, M. Keddam, A. Khalil, G. Maurin, H. Perrot, R. Rosset, M. Zidoune, Quartz crystal microbalance investigation of electrochemical calcium carbonate scaling, J. Electrochem. Soc. 145 (7) (1998).
[23] R. Ketrane, B. Saidani, O. Gil, L. Leleyter, F. Baraud, Efficiency of five scale inhibitors on calcium carbonate precipitation from hard water: effect of temperature and concentration, Desalination 249 (2009) 1397–1404.
[24] C. Gabrielli, M. Keddam, H. Perrot, A. Khalil, R. Rosset, M. Zidoune, Characterization of the efficiency of antiscale treatments of water part I, chemical processes, J. Appl. Electrochem. 26 (1996) 1125–1132.
[25] L.N. Plumber, E. Busenberg, The solubilities of calcite, aragonite and vaterite in CO_2—H_2O solutions between 0 and 90 °C, and an evaluation of the aqueous model for the system $CaCO_3$—CO_2—H_2O, Geochim. Cosmochim. Acta 46 (1982) 1011–1040.
[26] G. Gauthier, Y. Chao, O. Horner, O. Alos-Ramos, F. Hui, Application of the fast controlled precipitation method to assess the scale forming ability of raw river waters, Desalination 299 (2012) 89–95.
[27] A.G. Xyla, J. Mikroyannidis, P.G. Koutsoukos, The inhibition of calcium carbonate precipitation in aqueous media by organophosphorus compounds, J. Colloid Interface Sci. 153 (1992) 537–551.
[28] S.P. Gopi, V.K. Subramanian, K. Palanisamy, Aragonite-calcite-vaterite: a temperature influenced sequential polymorphic transformation of $CaCO_3$ in the presence of DTPA, Mater. Res. Bull. 48 (2013) 1906–1912.